Title
Nanotemplating of Biodegradable Polymer Membranes for Constant-Rate Drug Delivery

Journal
Advanced Materials, 22(21)

ISSN
0935-9648

Authors
Bernards, Daniel A
Desai, Tejal A

Publication Date
2010-06-04

DOI
10.1002/adma.200903439

Peer reviewed

ADVANCED MATERIALS
www.advmat.de

www.MaterialsViews.com

Nanotemplating of Biodegradable Polymer Membranes for Constant-Rate Drug Delivery

By *Daniel A. Bernards* and *Tejal A. Desai**

In recent years, advances in drug delivery have allowed for better control over dose and localized release, which has improved treatment efficacy and continues to lead to innovative therapies.[1] Nanoscale materials have been at the forefront of delivery strategies and continue to have significant impact.[2] While the majority of development has focused on various nanoparticle delivery vehicles, nanostructured substrates also have attractive properties for drug delivery associated with their structure. Initially developed theoretically[3] and first demonstrated in zeolites,[4] non-Fickian diffusion is possible in porous materials when the size of a diffusing species is comparable to the pore size of a material. The process is often referred to as ''single-file'' diffusion, which can lead to concentration-independent transport, and such zero-order release kinetics lead to nanostructured membranes that are particularly attractive for drug-delivery applications. Given relevant size scales, small-molecule delivery requires pores on the order of a nanometer, while macromolecule delivery requires pores on the order of a few tens of nanometers. As a result, careful material selection and design are of crucial importance in order to utilize this phenomenon for drug delivery.

Inorganic oxides have been among the first nanostructured materials to receive significant attention. For several decades, anodic growth of porous alumina has produced a wide range of pore sizes and densities; high pore densities ($>10^{10}\,cm^{-2}$) with pore sizes of the order of 10 nm can be achieved.[5] As a result, alumina membranes have been investigated for controlled release and immunoisolation.[6] More recently, advances in anodic growth of nanostructured titania have gained significant momentum and have been employed for a variety of therapeutic applications.[7] Various pore sizes have been demonstrated, including several examples down to 20–30 nm.[8] Alternatively, nanostructured silicon membranes have also been developed using contemporary microfabrication, which allows for precise control over the pore size.[9] While the pore density is comparatively low, sub-10-nm pores can be produced with a high degree of uniformity over large areas.[10] Given the established knowledge base of the semiconductor manufacturing, it is straightforward to modulate pore size and density through device design and fabrication conditions.

While nanostructured inorganic membranes benefit from uniform pore size and established processing techniques, these materials are not ideal for all drug-delivery applications. In particular, therapies that are not amenable to surgical implantation/excision or implant environments that require significant mechanical compliance are problematic for inorganic materials. An obvious alternative that avoids some of these drawbacks are polymeric materials: polymers have a wide range of chemical and mechanical properties, which allow design of flexible and potentially injectable devices. In addition, the use of biodegradable polymers enables devices that naturally degrade once their therapeutic payload is delivered.

Some of the earliest nanoporous polymers were formed by track-etching with high-energy radiation.[11] Established commercial examples exhibit pore sizes down to 15 nm and pore densities on the order of $10^9\,cm^{-2}$.[12] More recently, self-assembly techniques, such as block copolymers (BCP) and layer-by-layer (LbL) growth of polyelectrolytes, have emerged as popular routes to produce nanoscale features in polymers. Through appropriate design and processing, BCPs naturally phase-separate into nanoscale domains, which form nanostructured films upon selective dissolution of one phase.[13] This approach is capable of features comparable to that of inorganic materials. Unfortunately such films are restricted to a limited materials selection and oftentimes produce sub-100-nm-thick films,[14] although more recently thicker membranes have been demonstrated.[15] LbL assembly of polyelectrolytes is another popular approach to form nanostructured polymers. Sequential deposition of polycations and polyanions can be used to form films of arbitrary thickness, which may form nanostructures upon exposure to particular conditions.[16] In general, these materials have lower uniformity and pore formation is not well understood. In addition, LbL films are restricted to a bilayer structure of anionic and cationic polymers. Initially applied to antireflective coatings,[16] these films have also been utilized for controlled release of small-molecule therapeutics.[17] Both block copolymers and layer-by-layer assembly are attractive routes for nanostructure formation, but both approaches are restricted to a limited set of materials and application of these approaches to established commercially available materials is uncertain.

Ideally a nanoporous polymer would be biodegradable and flexible, allowing for injection, therapeutic delivery, and subsequent degradation. Such a device decouples delivery kinetics and device degradation. An excellent candidate material is poly(caprolactone) (PCL), as it has been shown to degrade in vivo over tens of months and maintains its structural integrity throughout the vast majority of the degradation timeframe.[18] Conventional microfabrication techniques have been successfully applied to PCL,[19] but such techniques are impractical for the required nanoscale resolution. Furthermore, while PCL nanofibers and nanoparticles have been developed,[20] little work has

[*] Prof. T. A. Desai, Dr. D. A. Bernards
Department of Bioengineering and Therapeutic Sciences and Department of Physiology
University of California, San Francisco
San Francisco, CA 94158 (USA)
E-mail: tejal.desai@ucsf.edu

DOI: 10.1002/adma.200903439

been focused on nanoporous films of PCL. The primary existing example of nanoporous PCL was fabricated using a phase-separation technique, where sub-100-nm pores were produced;[21] however, control over the pore size has not been demonstrated and pore densities are quite low ($\sim 10^8$ cm^{-2}). In general, there is need for an adaptable process to generate nanoporous polymeric films for application of arbitrary nanoporous polymers to drug-delivery systems.

Template-based fabrication is an established approach for pattern formation that is compatible with a variety of materials. Given its ease of processing and the commercial availability, alumina is a popular nanostructured template and has been applied to a host of materials, from metals to polymers.[22,23] In particular, nanoscale PCL rods have been successfully fabricated from alumina templates, demonstrating the viability of template-based fabrication with PCL;[23] however, in order to form a porous structure, a nanorod template is required. One nanorod material that has emerged in recent years is zinc oxide. Developed largely for photovoltaic applications, these rods can be grown using a simple hydrothermal process, which is capable of producing a variety of rod diameters.[24,25] In addition, microprinting has been used to pattern nanorod growth, providing control over template geometry.[25] Along with these reasons and the ability to etch zinc oxide in weakly acidic solutions, zinc oxide is an excellent candidate for use as a template in nanoporous polymer fabrication.

In this Communication we report the fabrication and characterization of nanoporous PCL films for application in drug delivery. Nanorod growth and a subsequent templating process is shown in Figure 1. PCL membranes were fabricated using zinc oxide nanorod templates fabricated using techniques established elsewhere.[26] Zinc oxide rods were grown hydrothermally in a dilute zinc acetate solution from a spin-cast zinc oxide layer. This resulted in growth of ZnO rods perpendicular to the seed layer with length of approximately 500 nm. Figure 1B shows a characteristic scanning electron microscope (SEM) image of ZnO nanorods, with average rod diameter of 23 ± 7 nm and typical rod densities of approximately 10^{10} rods cm^{-2}. Defects in the ZnO template are a significant concern for this technique, but their impact can be minimized with the appropriate processing environment.

Nanostructured PCL was formed by solution casting PCL onto nanostructured ZnO templates. A SEM of PCL-coated ZnO rods is shown in Figure 1C, which shows that the casting process does not adversely affect the nanostructures. Etching the ZnO template results in a nanoporous PCL thin film. Figure 1D shows a typical SEM of the nanostructured PCL, fabricated using this technique, with a pore size of 21 ± 7 nm and pore density of 5×10^9 pores cm^{-2}. Comparison of rod and pore diameter indicates good fidelity of pattern transfer. In general, defects in PCL films are associated with external particulate and can be identified in process prior to membrane or device testing: furthermore, spin-casting and solution processing have a prominent track record in semiconductor processing and defects associated with these processes can be minimized. Nanorod length variations in the ZnO template lead to a tradeoff between membrane thickness and pore density, where shorter rods may be covered when thicker PCL films are cast. Furthermore, any fracture or detachment of ZnO rods during handling and spin-casting will enhance this effect by decreasing rod length/density and consequently will decrease feature density from the template to the completed membrane. An artifact of the casting process, the majority of film roughness is associated with polymer-wetting ZnO rods, and consequently the exposed side of the polymer film is significantly rougher than the opposing side of the film. A porosity of ~2% can be calculated

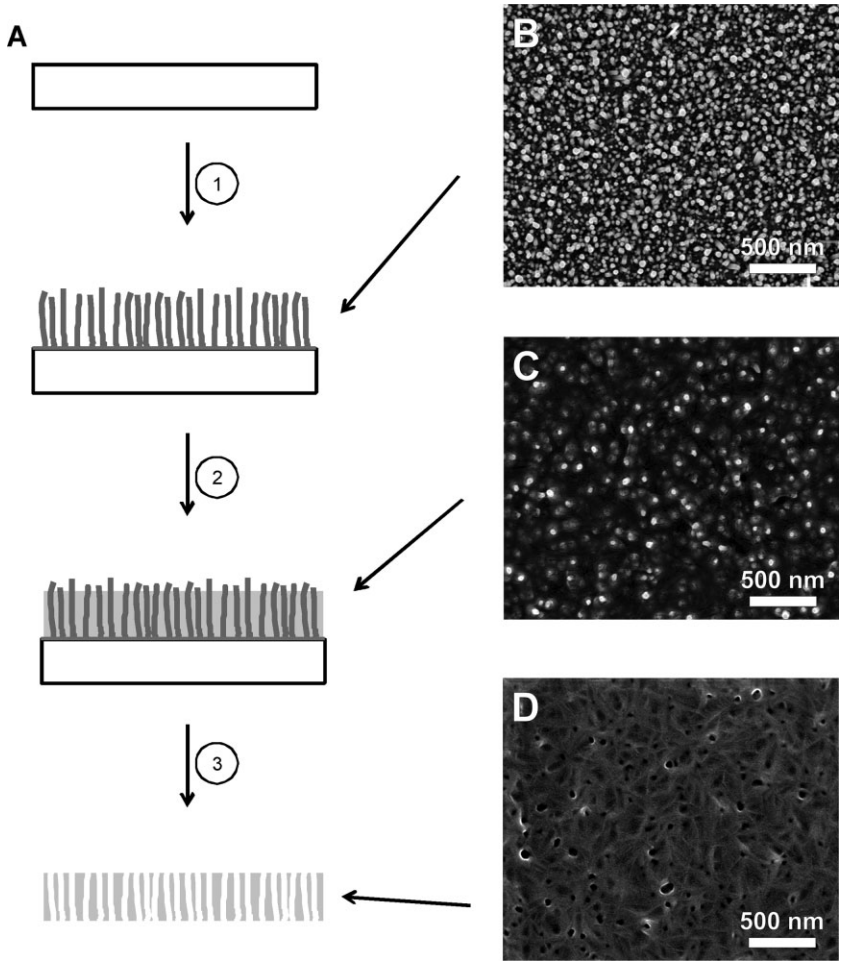

Figure 1. Fabrication of nanoporous poly(caprolactone). A) Processing sequence showing (1) zinc oxide growth, (2) casting of poly(caprolactone), and (3) etching of zinc oxide to produce nanostructured PCL. Characteristic SEM images show zinc oxide nanowires (B), PCL coated nanowires (C), and nanostructured PCL (D) (high-resolution versions of SEM images can be found in the Supporting Information).

based on the pore size and density, which is considerably lower than for other approaches; however, functional drug-delivery devices require a balance between pore density and structural integrity for robust and functional devices.

When compared with various nanoporous polymers,[12–17,19,21,27–29] this approach yields pore sizes that are comparable or smaller, although pore diameters less than 20 nm are difficult with this template choice. Cellulose membranes used for dialysis and ultrafiltration are capable of smaller pore sizes but have an irregular pore structure and are restricted in material selection.[28] Track-etch membranes are capable of thick membranes with highly uniform pore size but are known for low pore densities.[12] BCP techniques are also capable of dense sub-10-nm pores,[27] but the thickness of these membranes is limited and free-standing membranes usually have increased pore sizes.[15,29] While the approach demonstrated here typically does not obtain pore densities as high as BCP or LbL,[13–17] it has the distinct advantage of being applicable to essentially any polymer. Film thickness for this work is limited by the template thickness, which has an upper limit of approximately one micrometer for ZnO.[24] While thicker nanoporous membranes have been demonstrated, the nanoporous region of such membranes is only a fraction of the total membrane thickness,[15,21,29] so it is straightforward to obtain similar membranes with this approach by joining nanoporous PCL with macroporous supports. In general, pore size and density are currently a limitation of the template rather than the technique: using the above approach, a template with smaller pores or greater pore density would transfer directly to the polymer. Compared to existing fabrication techniques for nanostructured PCL films,[21] the technique produces smaller pores and higher pore densities.

Characteristic X-ray photoelectron spectra (XPS) of a nanostructured PCL film fabricated on a supporting silicon substrate is shown in Figure 2. Prominent carbon and oxygen peaks associated with PCL expectedly dominate the overall spectra. A high-resolution scan centered at the anticipated energy for zinc 2p electrons does not show a significant presence of zinc in the nanostructured film. This is a good indication that the etching process effectively removes the zinc oxide template. Because XPS probes surface composition, observation of silicon 2s and 2p peaks are evidence of directional porosity: silicon electrons can be detected by traversing the PCL's non-tortuous pores and avoid interacting with the PCL film (Figure 2B).

During the etching process, it is possible to float the PCL films off their supporting substrates and mount them in chambers for characterization of their transport properties. Sodium fluorescein (Fc) and fluorescein isothiocyanate-labeled bovine serum albumin (FITC-BSA) were selected as a characteristic small molecule and macromolecule, respectively, for diffusion experiments. Characteristic diffusion of Fc and FITC-BSA over time is shown in Figure 3. Fc, with a size of ~1 nm, much less than the PCL pore size, exhibits exponential release indicating first-order-type diffusion; because the molecular size is substantially less than the structural dimensions of the membrane, molecular diffusion is not constrained by the membrane structure. An exponential fit yields a time constant of 2.5 days, which corresponds to a diffusion coefficient of 2.4×10^{-10} cm^2 s^{-1}, assuming a perfect sink. This is several orders of magnitude less than the expected diffusion coefficient of free Fc in PBS (2.7×10^{-6} cm^2 s^{-1}).[30]

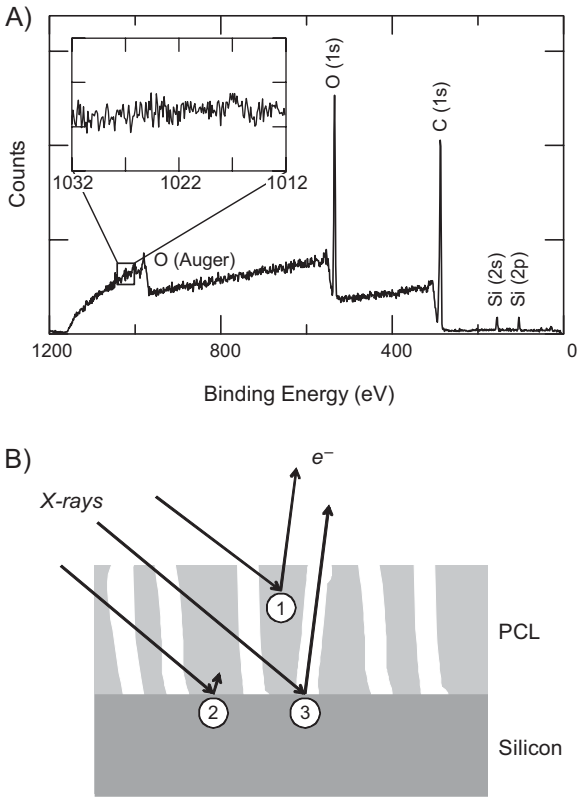

Figure 2. Chemical characterization of nanoporous PCL. A) XPS of nanoporous PCL on a silicon substrate with (inset) a high-resolution scan for presence of zinc (2p). B) Schematic image depicting the origin of Si XPS peaks, where electrons are either within the escape depth of the surface (detected) (1), reabsorbed due to their depth within the sample (undetected) (2), or escape through non-tortuous pores within film (detected) (3).

Due to the hydrophobic nature of PCL as well as the membrane geometry, one would suspect that the diffusivity of water-soluble molecules, such as Fc and FITC-BSA, will be decreased relative to free diffusion.

FITC-BSA was used as a model macromolecule; its size of ~7 nm[31] is on the order of the pore diameter. In this case, a constant release of 79 μg per day was observed, indicating zero-order behavior for the vast majority of release. This corresponds to a rate of approximately 33 BSA molecules exiting each pore every second. The rate observed for these membranes is comparable with existing technologies (Table 1);[9,10] although, due to significant differences in membrane geometry and chemical properties it is difficult to make meaningful comparisons between membrane types. Beginning day six, release of FITC-BSA becomes sublinear due to depletion of the source: as the source concentration decreases, the rate determined by the concentration gradient becomes less than the membrane-limited rate and behavior transistions to Fickian. This effect has been similarly described for microfabricated silicon membranes.[10]

To test the basic cellular compatibility, National Institute of Health (NIH) 3T3 fibroblast cells were grown on nanostructured PCL along with PCL, tissue culture polystyrene (TCPS), and glass for comparison. Two days after seeding, a MTT assay was

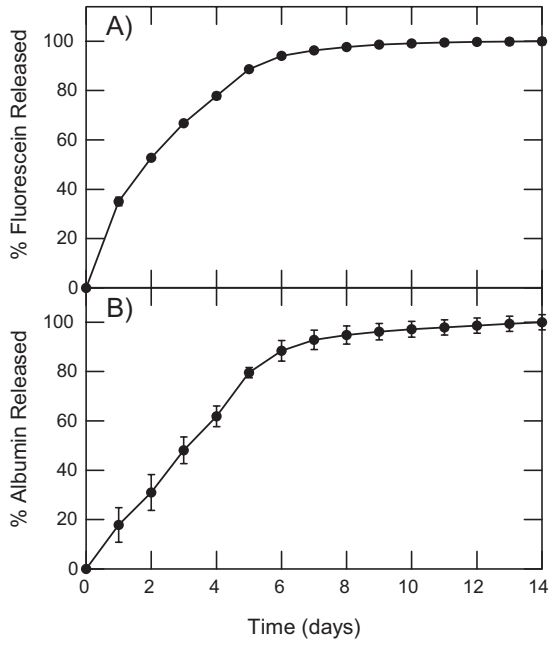

Figure 3. Characteristic diffusion through nanostructured membranes. A) Diffusion of a model small molecule, sodium fluorescein, and B) a model macromolecule, fluorescein isothiocyanate-labeled bovine serum albumin, through nanoporous PCL membranes (n = 3).

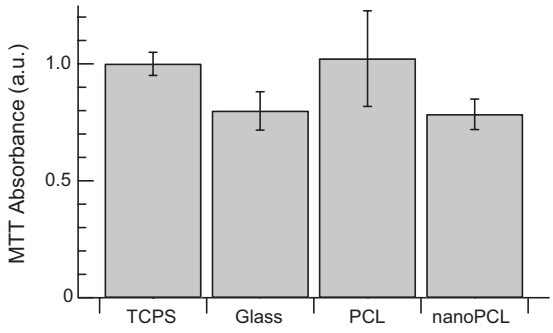

Figure 4. MTT assay of 3T3 fibroblast cells. Metabolic activity of fibroblasts grown on TCPS, glass, PCL, and nanostructured PCL normalized to TCPS (n = 4).

Table 1. Performance comparison for albumin diffusion through various nanoporous membranes.

Material	Nominal Pore Size [nm]	BSA Flux [mg day^{-1} mm^{-2}]	Reference
Whatman Anodisc (Alumina)	20	4.3	[9]
MF-Millipore (Cellulose)	25	2.5	[9]
Microfabricated Silicon	13	4.4	[10]
Template Fabricated PCL	23	0.9	–

performed to determine cellular metabolic activity. Figure 4 show the MTT results normalized relative to TCPS. Significant differences were not observed between the various substrates. This demonstrates that the templating process does not leave residual inorganic material that is cytotoxic. Basic cellular compatibility is critical for application of these materials in implantable drug-delivery devices.

In conclusion, this Communication demonstrated a template-based approach for the fabrication of nanostructured biodegradable polymers. Patterns were transferred with good fidelity from the ZnO template to the PCL membrane. Chemical characterization did not show traces of the template material, verifying effective removal of the template during the fabrication process. This fabrication procedure produced thin films than can be easily incorporated into flexible devices, which is a distinct advantage over rigid inorganic membranes. Diffusion of a macromolecule demonstrated zero-order release due to constrained diffusion, while small-molecule diffusion showed normal first-order release. For appropriately sized molecules, constrained diffusion can be used as an approach to achieve controlled release. A MTT assay with 3T3 fibroblasts indicated that the nanostructures did not adversely impact cellular growth. Controlled release of a model protein and basic cellular compatibility showed that these nanoporous films are promising candidates for therapeutic devices. In general, this approach to nanofabrication opens avenues for device design with a wider range of potential materials, allowing the development of a variety of nanostructure-based devices.

Experimental

All chemicals were obtained from Sigma–Aldrich (St. Louis, MO) unless otherwise noted. PCL membranes were fabricated using zinc oxide nanorod templates grown using techniques established elsewhere [26]. Zinc oxide rods were grown on glass substrates that were cleaned with a solution of sulfuric acid and hydrogen peroxide (3:1) for 30 min and subsequently rinsed with deionized water and dried with nitrogen. Substrates were exposed to an oxygen plasma (200W, 0.5 mTorr) for 5 min prior to spin-casting a zinc acetate ($ZnAc_2$) seed layer. A solution of $ZnAc_2$ (0.75 M) and ethanolamine (0.75 M) in 2-methoxyethanol was cast onto clean glass substrates at 1000 rpm for 60 seconds. Substrates were annealed on a hot plate at 400 °C for 30 min to convert $ZnAc_2$ into ZnO. Substrates were then placed in an aqueous $ZnAc_2$ solution (5 mM) at 85–90 °C for 4 h, replacing the growth bath once. Nanostructured PCL was formed by solution casting PCL in 2,2,2-trifluoroethanol (prepared by stirring at 60 °C until dissolved). PCL solutions were cast onto ZnO templates at 1000 rpm for 60 seconds and were heated to 130 °C to remove any excess solvent and to allow the PCL to intimately contact the template. ZnO templates were then etched with H_2SO_4 (10 mM) for 30 minutes. Typical films had an area of ~1 cm^2 and a thickness of 200–500 nm.

Characterization of material structures was performed using a FEI XL30 Sirion scanning electron microscope with field-emission gun source (FEI, Hillsboro, OR). ZnO-rod and PCL-pore diameters were determined using *ImageJ* analysis software (National Institutes of Health, USA). Chemical characterization was performed using a Surface Science Instruments S-Probe monochromatized X-ray photoelectron spectrometer, which uses Al Kα radiation (1486 eV) as a probe.

For diffusion experiments, PCL membranes were placed between two O-rings (2.5 mm diameter) and mounted into chambers. The interior (source) reservoir of the diffusion chamber was loaded with concentrated solute (50 μL; Fc or FITC-BSA) in phosphate buffered saline (PBS), and the exterior (sink) reservoirs were filled with PBS (500 μL). Diffusion chambers

were kept in an incubator at 37 °C on a shaker plate during the course of the experiment. The exterior reservoir was replaced daily and spectral absorbance was measured with a SpectraMAX 190 (Molecular Devices, Sunnyvale, CA) using 96-well plates (300 μL of solution) to determine the mass of solute diffused daily. Known solutions of Fc and FITC-BSA were used to calibrate absorbance to mass.

For cellular compatibility studies, NIH 3T3 fibroblast cells (5×10^3 cells cm^{-2}) were seeded in Dublecco's Modified Eagle's Medium (DMEM) with fetal bovine serum (10%) and penicillin/streptomycin solution (1%; Gibco, Grand Island, NY). Forty eight hours after seeding, a MTT assay was performed to determine cellular metabolic activity as determined from spectral absorbance.

Acknowledgements

The authors acknowledge Dr. Matthew Lloyd and Dr. Alex Mayer as well as the entire Desai Laboratory. This work was supported by the National Institutes of Health and the UC Discovery Program. All SEM imaging and XPS characterization was performed at the Stanford Nanocharacterization Laboratory through the Stanford CIS grant program. Supporting Information is available online from Wiley InterScience or from the author.

Received: November 22, 2009
Published online: April 7, 2010

[1] a) R. Langer, *Science* **1990**, *249*, 1527. b) T. M. Allen, P. R. Cullis, *Science* **2004**, *303*, 1818.
[2] R. Tong, D. A. Christian, L. Tang, H. Cabral, J. R. Baker, K. Kataoka, D. E. Discher, J. Cheng, *MRS Bull.* **2009**, *34*, 422.
[3] J. O. P. Chemistry, D. G. Levitt, *Phys. Rev. A* **1973**, *8*, 3050.
[4] K. Hahn, J. Karger, V. Kukla, *Phys. Rev. Lett.* **1996**, *76*, 2762.
[5] F. Keller, M. S. Hunter, D. L. Robinson, *J. Electrochem. Soc.* **1953**, *100*, 411.
[6] a) D. W. Gong, V. Yadavalli, M. Paulose, M. Pishko, C. A. Grimes, *Biomed. Microdevices* **2003**, *5*, 75. b) K. E. La Flamme, K. C. Popat, L. Leoni, E. Markiewicz, T. J. La Tempa, B. B. Roman, C. A. Grimes, T. A. Desai, *Biomaterials* **2007**, *28*, 2638.
[7] a) K. C. Popat, M. Eltgroth, T. J. La Tempa, C. A. Grimes, T. A. Desai, *Small* **2007**, *3*, 1878. b) M. Paulose, H. E. Prakasam, O. K. Varghese, L. Peng, K. C. Popat, G. K. Mor, T. A. Desai, C. A. Grimes, *J. Phys. Chem. C* **2007**, *111*, 14992. c) K. C. Popat, L. Leoni, C. A. Grimes, T. A. Desai, *Biomaterials* **2007**, *28*, 3188.
[8] a) E. Balaur, J. M. Macak, H. Tsuchiya, P. Schmuki, *J. Mater. Chem.* **2005**, *15*, 4488. b) H. Tsuchiya, J. M. Macak, L. Taveira, E. Balaur, A. Ghicov, K. Sirotna, P. Schmuki, *Electrochem. Commun.* **2005**, *7*, 576. c) G. K. Mor, K. Shankar, M. Paulose, O. K. Varghese, C. A. Grimes, *Nano Lett.* **2005**, *5*, 191.
[9] T. A. Desai, D. J. Hansford, M. Ferrari, *Biomol. Eng.* **2000**, *17*, 23.
[10] F. Martin, R. Walczak, A. Boiarski, M. Cohen, T. West, C. Cosentino, M. Ferrari, *J. Control. Release* **2005**, *102*, 123.
[11] P. B. Price, R. M. Walker, *J. Appl. Phys.* **1962**, *33*, 3407.
[12] Whatman Nucleopore Track Etch Membranes, http://www.whatman.com/NuclepreTrackEtchedMembranes.aspx (last accessed March 2010).
[13] F. S. Bates, *Science* **1991**, *251*, 898.
[14] R. Ruiz, H. M. Kang, F. A. Detcheverry, E. Dobisz, D. S. Kercher, T. R. Albrecht, J. J. de Pablo, P. F. Nealey, *Science* **2008**, *321*, 936.
[15] K. V. Peinemann, V. Abetz, P. F. W. Simon, *Nat. Mater.* **2007**, *6*, 992.
[16] J. Hiller, J. D. Mendelsohn, M. F. Rubner, *Nat. Mater.* **2002**, *1*, 59.
[17] M. C. Berg, L. Zhai, R. E. Cohen, M. F. Rubner, *Biomacromolecules* **2006**, *7*, 357.
[18] H. F. Sun, L. Mei, C. X. Song, X. M. Cui, P. Y. Wang, *Biomaterials* **2006**, *27*, 1735.
[19] D. K. Armani, C. Liu, *J. Micromech. Microeng.* **2000**, *10*, 80.
[20] a) A. Greiner, J. H. Wendorff, *Angew. Chem. Int. Ed.* **2007**, *46*, 5670. b) V. R. Sinha, K. Bansal, R. Kaushik, R. Kumria, A. Trehan, *Int. J. Pharm.* **2004**, *278*, 1.
[21] X. L. Zhang, H. Y. He, C. Yen, W. Ho, L. J. Lee, *Biomaterials* **2008**, *29*, 4253.
[22] H. Masuda, K. Fukuda, *Science* **1995**, *268*, 1466.
[23] S. L. Tao, T. A. Desai, *Nano Lett.* **2007**, *7*, 1463.
[24] L. E. Greene, M. Law, D. H. Tan, M. Montano, J. Goldberger, G. Somorjai, P. D. Yang, *Nano Lett.* **2005**, *5*, 1231.
[25] C. H. Wang, A. S. W. Wong, G. W. Ho, *Langmuir* **2007**, *23*, 11960.
[26] D. C. Olson, J. Piris, R. T. Collins, S. E. Shaheen, D. S. Ginley, *Thin Solid Films* **2006**, *496*, 26.
[27] U. Y. Jeong, D. Y. Ryu, J. K. Kim, D. H. Kim, X. D. Wu, T. P. Russell, *Macromolecules* **2003**, *36*, 10126.
[28] a) Millipore, MF-Millipore Membrane Filters, http://www.millipore.com/catalogue/module/c152 (last accessed March 2010). b) Spectrum Labs, Spectra/Por Biotech Dialysis Membranes, http://www.spectrapor.com/lit/420x10688x000.pdf (last accessed March 2010).
[29] F. Schacher, M. Ulbricht, A. H. E. Muller, *Adv. Funct. Mater.* **2009**, *19*, 1040.
[30] N. Periasamy, A. S. Verkman, *Biophys. J.* **1998**, *75*, 557.
[31] U. Bohme, U. Scheler, *Chem. Phys. Lett.* **2007**, *435*, 342.